IEEE Photonics Journal
An IEEE Photonics Society Publication

Open Access

One-Way Rotating Photonic Crystal Ring Resonator With High Quality Factor

Volume 10, Number 4, August 2018

Qiuyue Zhang
Xun Li, ***Senior Member, IEEE***

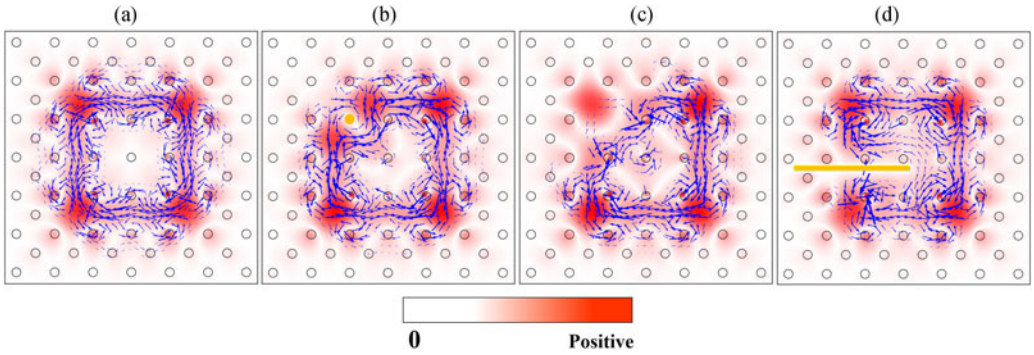

DOI: 10.1109/JPHOT.2018.2838324
1943-0655 © 2018 IEEE

IEEE photonics SOCIETY

IEEE

One-Way Rotating Photonic Crystal Ring Resonator With High Quality Factor

Qiuyue Zhang[1] **and Xun Li**[1,2] ***Senior Member, IEEE***

[1]Wuhan National Laboratory for Optoelectronics, Huazhong University of Science and Technology, Wuhan 430074, China
[2]Department of Electrical and Computer Engineering, McMaster University, Hamilton, ON L8S 4K2, Canada

DOI:10.1109/JPHOT.2018.2838324

Manuscript received April 3, 2018; revised May 11, 2018; accepted May 15, 2018. Date of publication May 18, 2018; date of current version May 29, 2018. Corresponding author: Xun Li (e-mail: lixun@mcmaster.ca).

Abstract: We propose a planar photonic crystal ring resonator consists of a looped single interface between a regular and a magneto-optical photonic crystal structure. The cavity modes are shown to possess the unidirectional rotation characteristics, and the rotating direction is determined by the direction of an externally applied magnetic field normal to the rotation plane. This unique unidirectional feature results in the realization of cavity with extremely high Q factor of 3.2×10^6, more than one order of magnitude higher than the previous report for cavity with the same ring size [Z. Qiang, W. Zhou, and R. A. Soref, "Optical add-drop filters based on photonic crystal ring resonators," Opt. Exp*ress*, vol. 15, no. 4, pp. 1823–1831, Feb. 2007]. As an example of its applications, we present a unidirectional channel-drop filter design based on the one-way rotating photonic crystal ring resonator. Our simulation result shows that a 96.7% backward dropping efficiency can be achieved by this filter.

Index Terms: Photonic crystal ring resonator, one-way rotating, high quality factor

1. Introduction

The anomalous one-way propagation property of magneto-optical photonic crystal (MOPC) waveguide has drawn much attention in recent years due to its potential applications in building optical isolators [2], circulators [3], [4], optical switches [5], splitters [6], [7] and slow light waveguides [8], [9]. Raghu and Haldane [10], [11] firstly predicted the existence of one-way electromagnetic modes in two-dimensional MOPC edge waveguide similar to the chiral edge states (CESs) found in integer quantum Hall effect (QHE). The modes are confined at the edge of MOPC and possess only positive (or only negative) group velocities, which is determined by the direction of the externally applied magnetic field. This idea was then confirmed by Wang *et al.* [12], [13] who presented realistic material designs and experimental verifications. Their work further demonstrated that such edge waveguides transmit electromagnetic waves without back-reflection even in the presence of an inserted metal reflector. Since the edge modes lie inside the light cone and will thus be leaky, a nonmagnetic metallic cladding or another regular photonic crystal has to be attached to the other side of the edge of the two-dimensional MOPC to avoid light scattering into the air. These studies spurred numerous subsequent theoretical [14]–[18] and experimental [19]–[21] investigations. The unidirectional transport property is unprecedented in photonics which promises to offer unique, robust designs and new device functionalities for photonic systems.

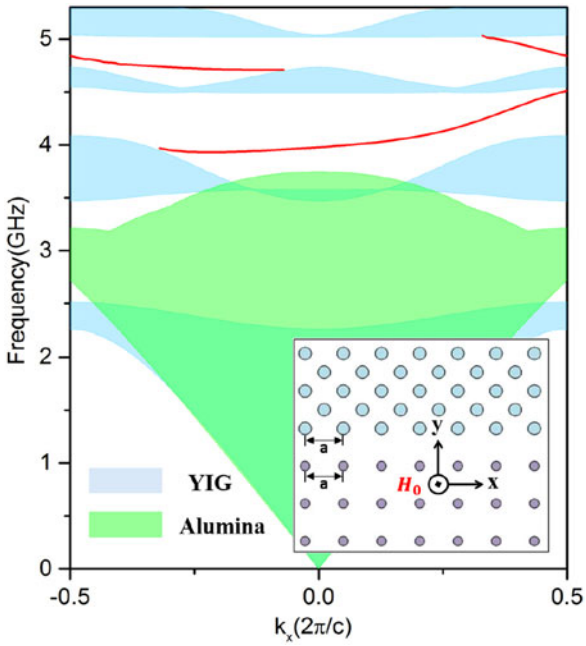

Fig. 1. Construction of the one-way waveguide. The waveguide consists of a square lattice of YIG rods (lower half plane) and a titled 45 degrees square lattice of Alumina rods (upper half plane), as shown in the inset. Calculated projected band diagram (green and blue areas). Included are the CESs (red curves) that exist at the interface between the MOPC and the Alumina PC. $\odot$ indicates an externally applied magnetic field in the $+z$ direction.

In this work, we propose a one-way in-plane photonic crystal ring resonator (PCRR) by curving the MOPC edge waveguide to form a closed loop. Owing to the ideal unidirectional propagation property in MOPC, such a resonator only support one-way rotating waves and is totally different from the PCRR studied before [1], [22]. In addition, by reversing the direction of the externally applied magnetic field, the rotation direction will be reversed accordingly. Coupled with two extra one-way edge waveguides, the bus and the drop channel, a unidirectional photonic crystal (PC) channel-drop filter (CDF) can be realized. In conventional all-dielectric PC CDF designs [1], [23], [24], light propagating in either direction sees the identical dropping function, whereas our proposed unidirectional CDF can selectively process the light signal propagating along a unique direction. In previous reports [25], [26], the unidirectional CDFs are based on point defect PC cavities. The PC point cavities are not robust against scattering from disorders or defects. It is difficult to avoid the performance degradation induced by fabrication imperfections or environmental changes. In our proposed one-way rotating resonator based nonreciprocal CDF, the PCRR is robust against scattering from disorders or defects. This feature ensures that the design is tolerant of fabrication imperfections.

The followed description of this work is organized as follows: the idea of edge modes in the unidirectional waveguide is briefed and the design of one-way rotating PCRR is then introduced in the next section. The quality factors of the one-way rotating PCRR is studied in Section 3, followed by the design of a one-way rotating PCRR based CDF in Section 4. All our simulation results are obtained by exploiting the finite element method (FEM).

2. Unidirectional Waveguide and One-Way Rotating Ring Resonator

The one-way waveguide is depicted in the inset in Fig. 1. The lower half plane is a square lattice MOPC consisting of Yttrium-Iron-Garnet (YIG) rods. The lattice constant is $a = 38.69$ mm and the radius of the rod is $r_1 = 0.11\,a$. The relative dielectric constant of the rods is 15 with a loss tangent

of 0.0002. With an external magnetic field applied in the $+z$ direction, a strong gyromagnetic anisotropy is induced with the permeability tensor taking the form of

$$\mu = \begin{bmatrix} \mu_r & i\mu_k & 0 \\ -i\mu_k & \mu_r & 0 \\ 0 & 0 & 1 \end{bmatrix} \mu_0 \tag{1}$$

where

$$\mu_r = 1 + \frac{\omega_m(\omega_0 + i\alpha\omega)}{(\omega_0 + i\alpha\omega)^2 - \omega^2}, \quad \mu_k = \frac{\omega_m\omega}{(\omega_0 + i\alpha\omega)^2 - \omega^2} \tag{2}$$

Here $\omega_0 = \mu_0\gamma H_0$ is the precession resonance frequency in the externally applied magnetic field H_0; $\omega_m = \mu_0\gamma M_s$ is the characteristic frequency at the saturation magnetization M_s of the YIG; ω is the angular frequency of the microwave field; μ_0 denotes the permeability of free space; and γ is the gyromagnetic ratio; the loss factor $\alpha = \mu_0\gamma\Delta H/(2\omega)$ is related to the line width ΔH of the susceptibility curve near the resonance. If the direction of externally applied magnetic field is reversed, both H_0 and M_s will change signs, consequently ω_0, ω_m and α change signs accordingly. Equation (2) then shows that μ_r remains unchanged, butμ_k changes its sign [27]. The YIG has a saturation magnetization $M_s = 1.42 \times 10^5$ A·m^{-1} and a resonance linewidth $\Delta H = 7.95 \times 10^2$ A·m^{-1}. The externally applied magnetic field is set to $H_0 = 1.27 \times 10^5$ A·m^{-1}. To restrict the edge modes near the interface of the MOPC, a titled 45 degrees square lattice of regular PC consisting of Alumina rods ($\varepsilon = 10\varepsilon_0$, $r_2 = 0.115a$) at the upper half plane is used to match the bandgap frequency. Frequency band gap in the MOPC overlaps with that in the Alumina PC. Therefore, the excited edge mode undergoes exponentially decay into both structures and is confined to the interface.

The projected band diagram of transverse magnetic (TM) modes with an external magnetic field applied in the $+z$ direction are plotted in Fig. 1, where the red curves correspond to the CESs that exist at the interface between the MOPC and the Alumina PC, and the shadow blue and green regions are for MOPC and Alumina PC respectively. The unidirectionality of the CES can be seen from the slope (group velocities) of the waveguide dispersions. As illustrated in Fig. 1, at frequencies within the second bandgap (correspond to frequency interval from 4.01 GHz to 4.45 GHz), the upper boundary of MOPC supports only forward propagation waves as it has only positive group velocities. Whereas at frequencies within the third bandgap (correspond to frequency interval from 4.81 GHz to 5.04 GHz), the upper boundary of MOPC supports only backward propagation waves as it has only negative group velocities. It is noteworthy that the transmission direction of electromagnetic waves in the one-way waveguide is controlled by the external magnetic field. As long as the sign of the magnetic field is reversed, the propagation is switched to the opposite direction accordingly.

Following the one-way transmission property of the aforementioned structure, we propose a planar one-way rotating PCRR as depicted in Fig. 2. The ring is formed by a looped single interface between two types of PC, the inner layered MOPC and the outer layered Alumina PC, with the air as the background. The cavities with different ring sizes are analyzed, the 2×2 structure shows the best performance, followed by the 3×3 structure, the 4×4 structure, etc. Since our design goal of the PCRR is a CDF, to obtain a desired effective coupling between the cavity and input/output waveguides, we have to choose the 3×3 cavity, as a smaller sized 2×2 design suffers from a higher insertion loss from the input to the output port. We choose a calculation area of 10 (x axis) $\times$ 10 (y axis) lattice periods, which is the same ring size as previously reported PCRR [1]. Contrary to an ordinary PCRR that supports both clockwise and counter-clockwise propagated modes, our proposed resonator supports only clockwise (or counter-clockwise) propagated modes as it has only positive (or only negative) group velocities. To illustrate the performance of the one-way rotating PCRR, the electric field patterns (color scale) and the corresponding Poynting vectors (blue arrows) distributions of the cavity modes within the spectral range of the second bandgap are shown in Fig. 3. Under an externally applied magnetic field in the $+z$ direction, the power flow circulates only in the clockwise direction as shown in Fig. 3(a). Under the reversed externally applied magnetic field in the $-z$ direction, the power flow circulates in the counter-clockwise direction as shown in

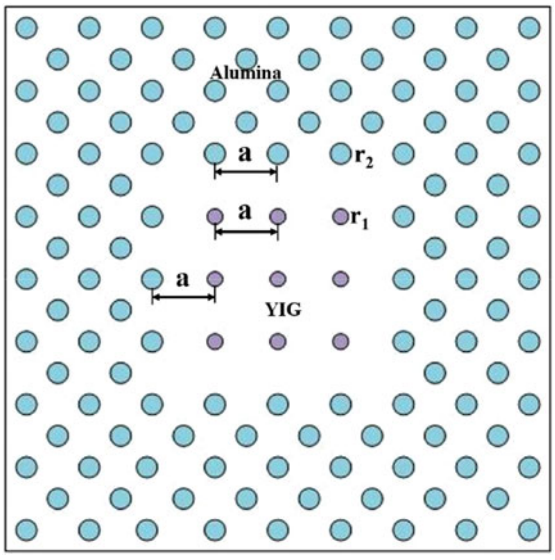

Fig. 2. Schematic structure of the one-way rotating photonic crystal ring resonator. Blue ones denote Alumina rods and purple ones denote YIG rods.

Fig. 3(b). This unique feature of the resonator attributes to the nonreciprocal effect of the MOPC. The one-way rotating PCRR modes in the third bandgap would be rotating in a totally opposite way. As shown in Fig. 4(a), under an external magnetic field applied along the $+z$ direction, the power flow circulates in the counter-clockwise direction, whereas for reversely applied magnetic field along the $-z$ direction, the power flow circulates in the clockwise direction as shown in Fig. 4(b).

3. Quality Factor

The quality factor of a cavity is determined by the energy loss per cycle versus the energy stored. In conventional PCRR, extrinsic scattering loss resulting from random fabrication variations, such as disorder and surface roughness, is considered as one of the most critical hurdles. Whereas in our proposed PCRR design, there are no counter propagating modes at the same frequencies as the one-way modes. This enables light to circumvent the disorders without inducing scattering loss. Taking loss factor of the YIG material into consideration, the quality factors versus the corresponding resonant frequencies are shown in Fig. 6(a), with a high quality factor of 3.2×10^6 and the effective edge-length (L_{eff}) of $\sim 2.1\lambda$ is obtained in our simulation. For comparison, the quality factors of the conventional PCRR with the same ring size as one-way rotating PCRR is shown in Fig. 6(b). It can be found that the quality factor of the unidirectional PCRR is more than one order of magnitude higher than the conventional PCRR [1]. This high quality feature is highly desirable for spectral selectivity and frequencies adjustment in the filter and switch design. To demonstrate the robustness of the one-way rotation, three types of defects are investigated in the resonator, including replacing a YIG rod with a Copper rod of the same size, removing a YIG rod and leaving with an air hole, inserting a metal reflector in the ring as shown in Fig. 5. In all three cases, the power flow simply circle around the obstacles without any backward scattering. Our simulation show that the corresponding quality factors are not substantially affected by these obstacles as illustrated in Fig. 6(a). While for conventional PCRR, such drastic obstacles would introduce strong backscattering. As shown in the Fig. 6(b), the quality factors of the conventional PCRR decrease by one order of magnitude when the three kinds of defects are introduced in the resonator.

The one-way rotating PCRR can be tailored further to purse larger quality factors. By adjusting the radius of the YIG rods (outlined in red in the inset of Fig. 7), a higher quality factor of 4.3×10^6 and the effective edge-length of $\sim 2.1\lambda$ is obtained for $r_3 = 0.1\,a$ as shown in Fig. 7.

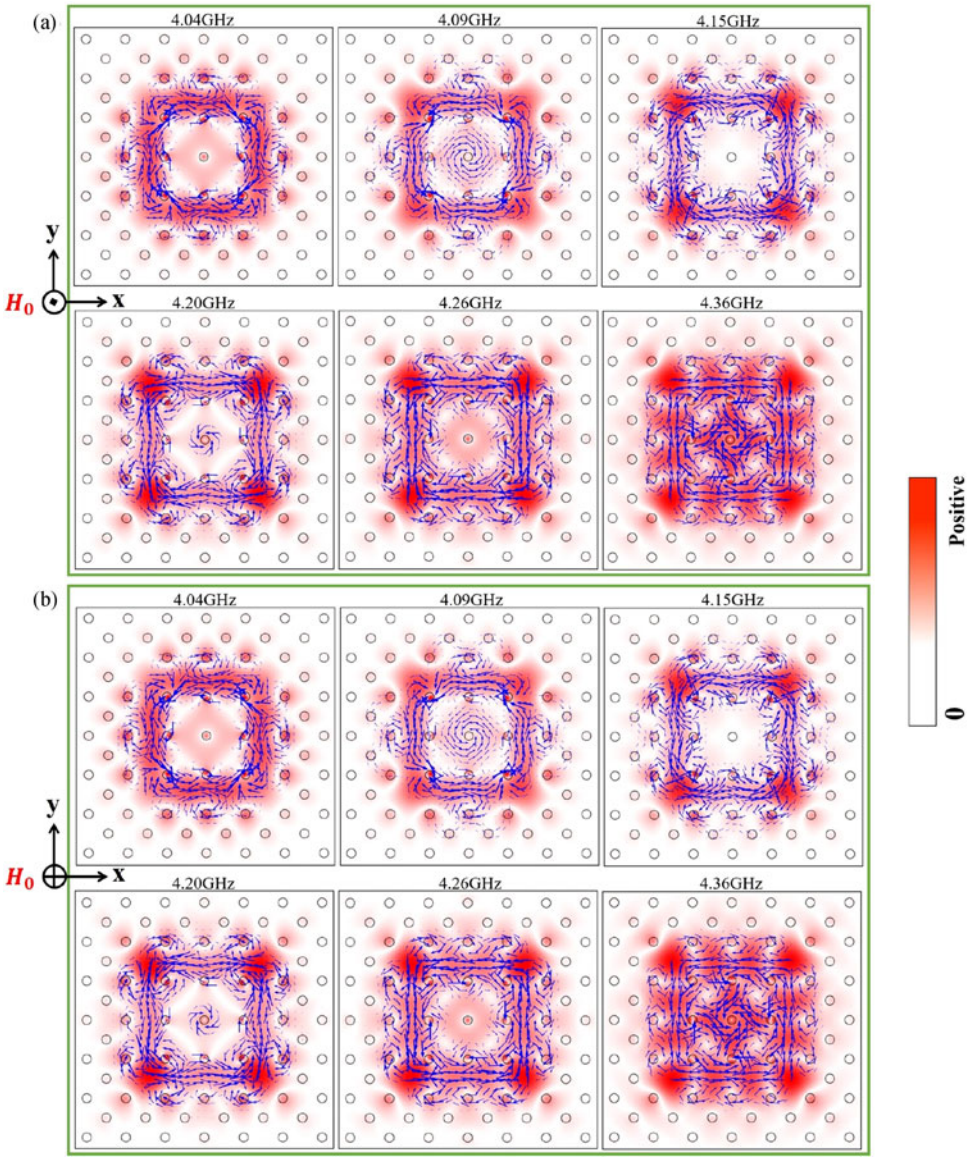

Fig. 3. The electric field patterns for E_z (color scale) and the Poynting vectors distributions (blue arrows) corresponding to six resonant frequencies within the second bandgap: 4.04 GHz, 4.09 GHz, 4.15 GHz, 4.20 GHz, 4.26 GHz, 4.36 GHz (a) with an external magnetic field applied along the $+z$ direction and (b) with an external magnetic field applied along the $-z$ direction. Colorbar represents the field strength.

4. One-Way Rotating PCRR Based CDF

As an example of applications of the one-way rotating PCRR, we present a PCRR based unidirectional CDF. The schematic structure is shown in Fig. 8. The CDF is composed of three main parts: a PCRR and two one-way waveguides as the bus waveguide (the upper one) and the drop waveguide (the lower one). Note that the CDF has four ports: port A (the input terminal), port B (the output terminal), port C (the backward dropping terminal) and port D (the forward dropping terminal). The performance of a CDF is determined by the transfer efficiency between the bus and drop waveguides. The electric field pattern at the resonant frequency is shown in Fig. 9(a). All the energy is transferred along the backward direction of the drop waveguide. The corresponding normalized transmission spectra for three output ports B, C, and D in the CDF are illustrated in

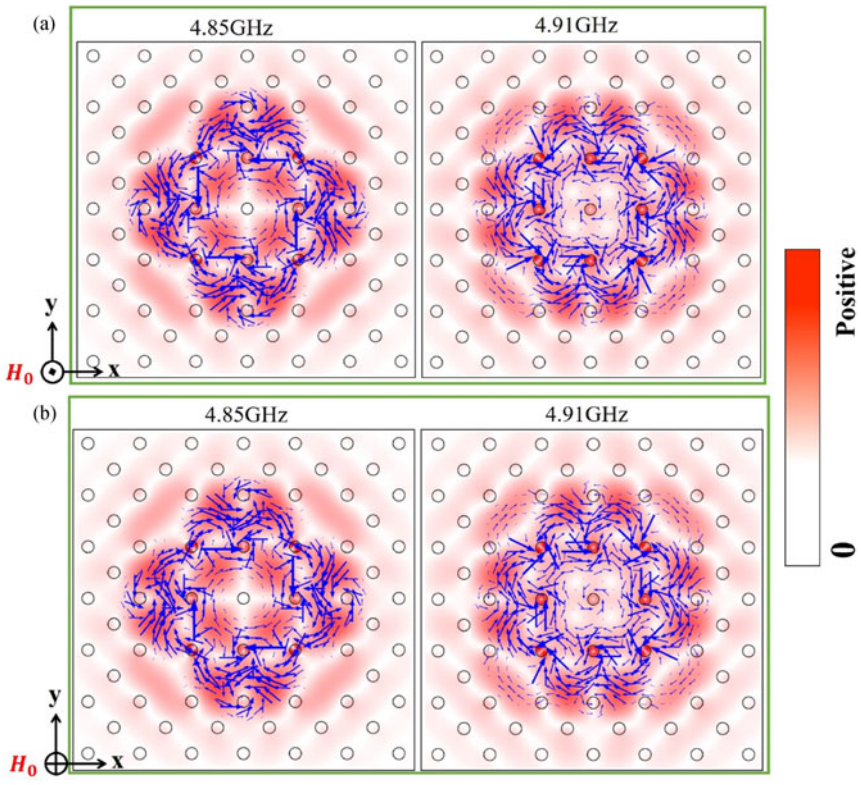

Fig. 4. The electric field patterns for E_z (color scale) and the Poynting vectors distributions (blue arrows) corresponding to two resonant frequencies within the third bandgap: 4.85GHz, 4.91GHz (a) with an external magnetic field applied along the $+z$ direction and (b) with an external magnetic field applied along the $-z$ direction. Colorbar represents the field strength.

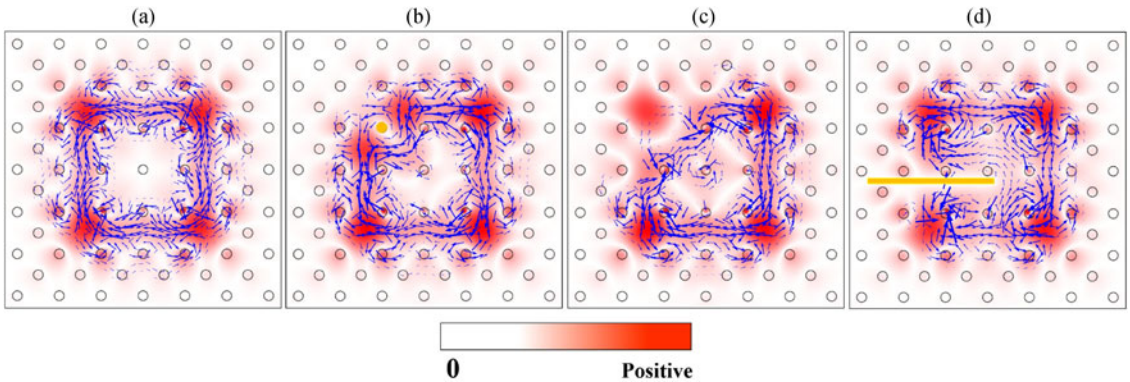

Fig. 5. The electric field patterns for E_z (color scale) and the Poynting vectors distributions (blue arrows) in the one-way PCRR (a) without introducing defects; (b)–(d) with three different types of defects: (b) replacing a YIG rod with a Copper rod (the yellow circle) of the same size, (c) removing a YIG rod and leaving with an air hole, and (d) inserting a metal reflector (the yellow rectangle) in the ring. Colorbar represents the field strength.

Fig. 9(b). Due to the absence of forward-propagating modes in the drop waveguide, there is a complete absence of field in the forward dropping terminal D over the entire frequency range. With 96.7% drop efficiency is achieved at the resonant frequency and the corresponding insertion loss is 0.33 dB. The quality factor for the CDF is around 5000, which is sufficiently large for practical demand [24]. The discrepancy between the quality factor of the PCRR and the CDF is mainly

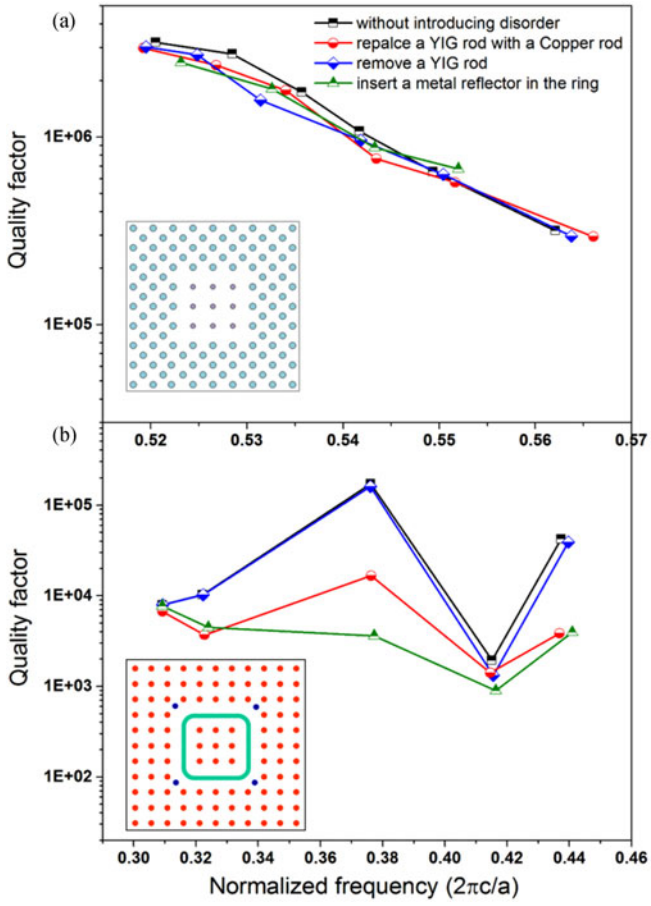

Fig. 6. Quality factors as a function of the resonant frequencies corresponding to four different cases in Fig. 5 for (a) the one way rotating PCRR and (b) the conventional PCRR with the same ring size as the one-way rotating PCRR. The left-bottom insets in (a), (b) show the corresponding geometric construction.

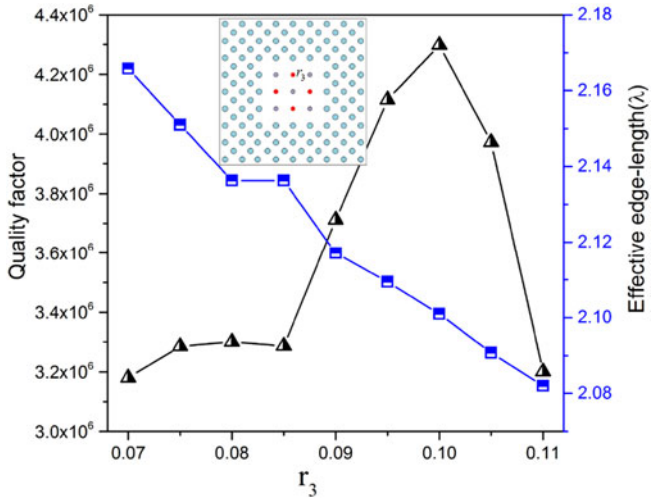

Fig. 7. Quality factors and effective edge-length of the tailored one-way rotating PCRR as a function of the rod radius r_3. The inset shows the new configuration of the resonator, the radius of the YIG rods outlined in red is reduced to r_3.

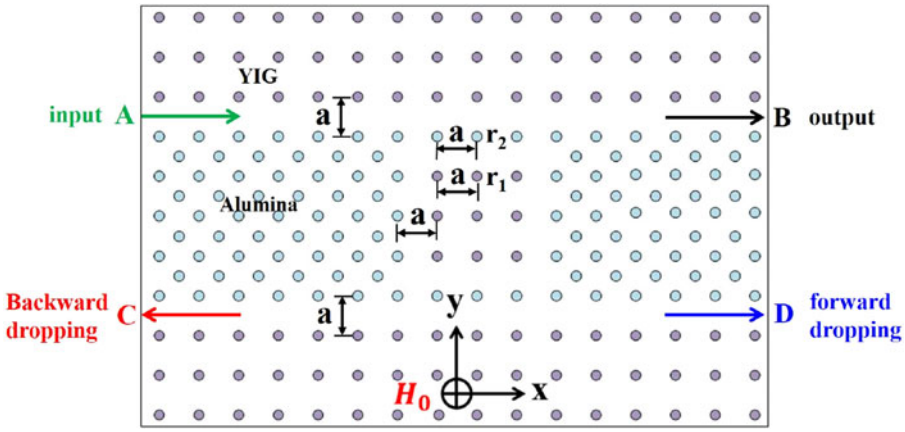

Fig. 8. Schematic structure of the PCRR based CDF. Blue rods denote Alumina PC and purple rods denote MOPC, ⊕ indicates an externally applied magnetic field in the $-z$ direction.

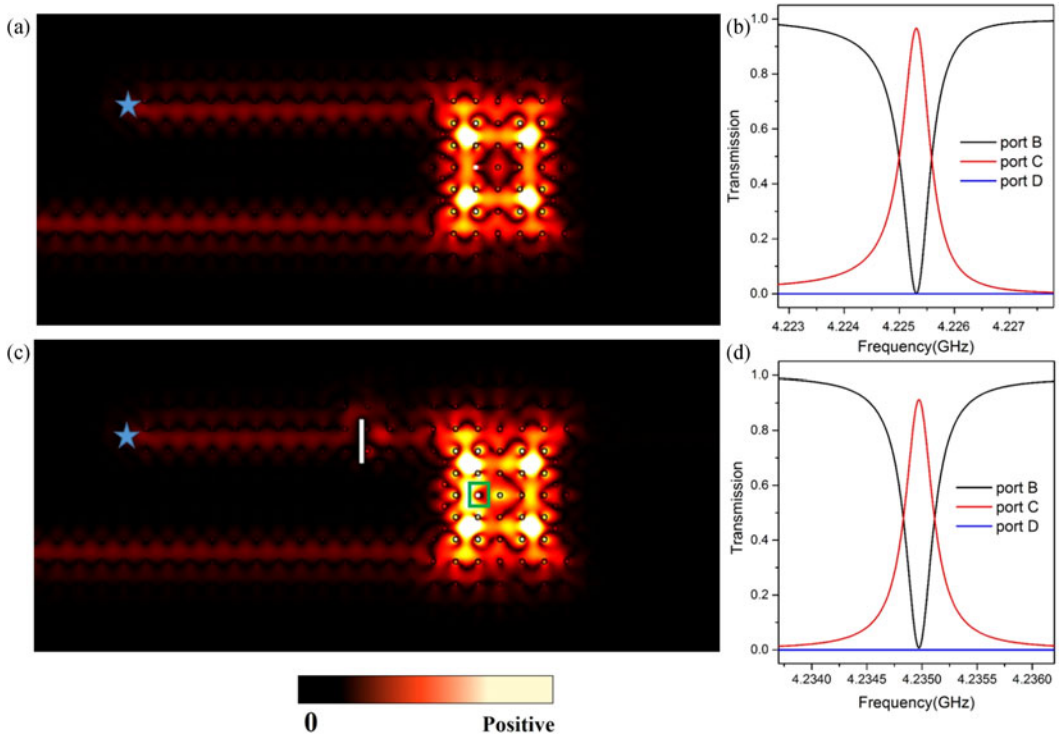

Fig. 9. (a) The electric field pattern (color scale) at the resonant frequency and (b) the normalized transmission spectra at three output ports B, C and D for CDF without introducing obstacles. (c) The electric field pattern at the resonant frequency and (d) the normalized transmission spectra at three output ports B, C and D for CDF with a slab of metal reflector of thickness 0.2a and width 2a (indicated by a white rectangle) inserted into the bus waveguide and a YIG rod in the resonator replaced by a Copper rod of the same size (circled in a green rectangle). The excitation source is indicated by a blue star. Colorbar represents the field strength.

due to the weak coupling between the waveguide and cavity. With further optimization such as increasing the coupling distance between the cavity and the waveguides, tuning the PCRR cavity quality factor (the rods sizes and location adjustment), much higher quality factors can be obtained. When a slab of metal reflector with thickness 0.2a and width 2a (indicated by a white rectangle) is inserted in the bus waveguide and a YIG rod in the resonator is replaced by a Copper rod of

the same size, the light can navigate around the disorders with perfect transmission as verified in Fig. 9(c). In a conventional CDF, such a drastic barrier would introduce strong backscattering and completely block the guided mode. In the unidirectional CDF, the inserted metal reflector results only in a change of the phase of the transmitted radiation, with no reduction in amplitude. This happens because the defect creates a new interface waveguide between the metal reflector and the MOPC. The corresponding normalized transmission spectra for three output ports B, C, and D in the CDF are illustrated in Fig. 9(d). With 91.3% drop efficiency is achieved at the resonant frequency and the corresponding insertion loss of is 0.91 dB. The performance of the device is not substantially affected by the disorders ensures that the design is tolerant of fabrication imperfections or environmental changes.

5. Conclusion

In this paper, a PCRR with one-way rotating property is proposed based on the unidirectionality and robustness of the CES. The rotation direction can be manipulated by the direction of the externally applied magnetic field. A high quality factor of 3.2×10^6 is obtained, which is one order of magnitude higher than previously reported cavities with the same ring size. By adjusting the radius of certain YIG rods, much larger quality factor of 4.3×10^6 is obtained. In addition, our simulation results demonstrate that the one-way rotation are immune to scattering from disorder ensures that the design is tolerant of fabrication imperfections. And the corresponding quality factors are not substantially affected by the introduced obstacles. A unidirectional CDF design based on the one-way rotating PCRR is proposed. With 96.7% drop efficiency is achieved in the CDF and the result is not substantially affected in the presence of disorders.

References

[1] Z. Qiang, W. Zhou, and R. A. Soref, "Optical add-drop filters based on photonic crystal ring resonators," *Opt. Exp.*, vol. 15, no. 4, pp. 1823–1831, Feb. 2007.

[2] Z. Yu and S. Fan, "Complete optical isolation created by indirect interband photonic transitions," *Nature Photon.*, vol. 3, no. 2, pp. 91–94, Jan. 2009.

[3] W. Qiu, Z. Wang, and M. Soljačić, "Broadband circulators based on directional coupling of one-way waveguides," *Opt. Exp.*, vol. 19, no. 22, pp. 22248–22257, Oct. 2011.

[4] Z. Wang and S. Fan, "Optical circulators in two-dimensional magneto-optical photonic crystals," *Opt. Lett.*, vol. 30, no. 15, pp. 1989–1991, Aug. 2005.

[5] X. Zang and C. Jiang, "Edge mode in nonreciprocal photonic crystal waveguide: Manipulating the unidirectional electromagnetic pulse dynamically," *J. Opt. Soc. Amer. B*, vol. 28, no. 3, pp. 554–557, Mar. 2011.

[6] C. He *et al.*, "Tunable one-way cross-waveguide splitter based on gyromagnetic photonic crystal," *Appl. Phys. Lett.*, vol. 96, no. 11, Mar. 2010, Art. no. 111111.

[7] Z. Wang, L. Shen, Z. Yu, X. Zhang, and X. Zheng, "Highly efficient photonic-crystal splitters based on one-way waveguiding," *J. Opt. Soc. Amer. B*, vol. 30, no. 1, pp. 173–176, Jan. 2013.

[8] T. Baba, "Slow light in photonic crystals," *Nature Photon.*, vol. 2, pp. 465–473, Aug. 2008.

[9] Y. Yang, Y. Poo, R. X. Wu, Y. Gu, and P. Chen, "Experimental demonstration of one-way slow wave in waveguide involving gyromagnetic photonic crystals," *Appl. Phys. Lett.*, vol. 102, no. 23, May 2013, Art. no. 231113.

[10] F. D. Haldane and S. Raghu, "Possible realization of directional optical waveguides in photonic crystals with broken time-reversal symmetry," *Phys. Rev. Lett.*, vol. 100, no. 1, Jan. 2008, Art. no. 013904.

[11] S. Raghu and F. D. M. Haldane, "Analogs of quantum-Hall-effect edge states in photonic crystals," *Phys. Rev. A*, vol. 78, no. 3, Sep. 2008, Art. no. 033834.

[12] Z. Wang, Y. Chong, J. D. Joannopoulos, and M. Soljacic, "Observation of unidirectional backscattering-immune topological electromagnetic states," *Nature*, vol. 461, no. 7265, pp. 772–775, Oct. 2009.

[13] Z. Wang, Y. D. Chong, J. D. Joannopoulos, and M. Soljacic, "Reflection-free one-way edge modes in a gyromagnetic photonic crystal," *Phys. Rev. Lett.*, vol. 100, no. 1, Jan. 2008, Art. no. 013905.

[14] L. Lu, L. Fu, J. D. Joannopoulos, and M. Soljac˘ic, "Weyl points and line nodes in gyroid photonic crystals," *Nature Photon.*, vol. 7, pp. 294–299, Mar. 2013.

[15] L. Lu, J. D. Joannopoulos, and M. Soljačić, "Topological Photonics," *Nature Photon.*, vol. 8, pp. 821–829, Oct. 2014.

[16] S. A. Skirlo, L. Lu, and M. Soljacic, "Multimode one-way waveguides of large Chern numbers," *Phys. Rev. Lett.*, vol. 113, no. 11, Sep. 2014, Art. no. 113904.

[17] X. Ao, Z. Lin, and C. T. Chan, "One-way edge mode in a magneto-optical honeycomb photonic crystal," *Phys. Rev. B*, vol. 80, no. 3, Jul. 2009, Art. no. 033105.

[18] A. B. Khanikaev, S. H. Mousavi, W. K. Tse, M. Kargarian, A. H. MacDonald, and G. Shvets, "photonic topological insulators," *Nature Mater.*, vol. 12, pp. 233–239, Dec. 2013.

[19] Y. Poo, R. X. Wu, Z. Lin, Y. Yang, and C. T. Chan, "Experimental realization of self-guiding unidirectional electromagnetic edge states," *Phys. Rev. Lett.*, vol. 106, no. 9, Mar. 2011, Art. no. 093903.
[20] M. Hafezi, S. Mittal, J. Fan, A. Migdall, and J. M. Taylor, "Imaging topological edge states in silicon photonics," *Nature Photon.*, vol. 7, pp. 1001–1006, Oct. 2013.
[21] M. C. Rechtsman *et al.*, "Photonic Floquet topological insulators," *Nature*, vol. 496, no. 7444, pp. 196–200, Apr. 2013.
[22] Y. Zhang *et al.*, "High-quality-factor photonic crystal ring resonator," *Opt. Lett.*, vol. 39, no. 5, pp. 1282–1285, Mar. 2014.
[23] S. Fan, P. R. Villeneuve, and J. D. Joannopoulos, "Channel drop filters in photonic crystals," *Opt. Exp.*, vol. 3, no. 1, pp. 4–11, Jul. 1998.
[24] D. Stieler, A. Barsic, R. Biswas, G. Tuttle, and K. M. Ho, "A planar four-port channel drop filter in the three-dimensional woodpile photonic crystal," *Opt. Exp.*, vol. 17, no. 8, pp. 6128–6133, Apr. 2009.
[25] J. X. Fu, J. Lian, R. J. Liu, L. Gan, and Z. Y. Li, "Unidirectional channel-drop filter by one-way gyromagnetic photonic crystal waveguides," *Appl. Phys. Lett.*, vol. 98, no. 21, 2011, Art. no. 211104.
[26] K. Tao, J. J. Xiao, and X. Yin, "Nonreciprocal photonic crystal add-drop filter," *Appl. Phys. Lett.*, vol. 105, no. 21, 2014, Art. no. 211105.
[27] D. M. Pozar, *Microwave Engineering*. Hoboken, NJ, USA: Wiley, 2012.